Presented at the 35th European PV Solar Energy Conference and Exhibition, 24-28 September 2018, Brussels, Belgium

DEFECTS IN EPITAXIALLY GROWN SILICON WAFERS CAUSING LIFETIME PATTERNS

Marion Drießen, Patrick Beu, Friedemann D. Heinz, Tobias Fehrenbach, Elke Gust, Florian Schindler, Stefan Janz
Fraunhofer Institute for Solar Energy Systems (ISE)
Heidenhofstrasse 2, 79110 Freiburg, Germany

ABSTRACT: Epitaxially grown silicon wafers (EpiWafers) have the potential of gaining high electrical quality while production costs can be significantly reduced compared to conventional wafers. High efficiencies are already reported for solar cells made of EpiWafers yet defects originating from the specific production sequence are limiting their quality. Photoluminescence imaging shows line patterns of high recombination activity. A further reduced lifetime is visible in square shaped features often positioned at crossing points of the lines. Those features correspond mainly to stacking faults with polycrystalline inclusions, similar square shaped features beside lines to regular stacking faults. Micro photoluminescence measurements reveal that the lines consist of agglomerations of spots with high recombination activity. In the areas with those spots threading dislocations can be found on defect etched samples in a number exceeding the number of spots. We explain all observations by dislocation mediated impurity aggregation and precipitation.
Keywords: EpiWafer, Defects, kerf-less wafering

1 INTRODUCTION

Epitaxially grown silicon wafers (EpiWafers) are a promising alternative for standard wafers since material and energy consumption are significantly reduced leading to reduced overall costs per watt peak if the quality is comparable to standard wafers. High minority charge carrier lifetimes of up to 7 ms are already reported for EpiWafers [1]. Also efficiencies of up to 23 % for solar cells have been reported [2]. But still the specific production sequence leads to special defects that limit the quality of EpiWafers [3,4,5]. The fabrication contains epitaxial growth of the final wafer on top of a reorganized porous silicon double layer that acts as template for growth and predetermined breaking point for detachment. At nucleation sites on the template stacking faults grow along four {111} planes forming inverted pyramids within the epitaxial layer referred to SF in the following. Hence, apex of the SFs is at the side of the interface and the according base is exposed to the wafer's surface. The SFs can also contain polycrystalline inclusions bordered by the same {111} planes as SFs and therefore are called polySFs.

In [3] lifetime images exhibiting line patterns of reduced lifetime areas are reported. At crossing point of those lines of reduced lifetime often polySFs are positioned.

In the following the correlation of these lines and polySFs is investigated in more detail using photoluminescence measurements with a higher resolution. Afterwards the structure within these lines and the origin of the lifetime reduction are discussed. For this purpose micro photoluminescence measurements with an even higher resolution are compared with the defect structure in the region around polySFs. After looking at local strain around an exemplary polySF with Raman measurement a model is presented which can explain the origin of the lifetime pattern.

2 EXPERIMENTAL PROCEDURE

2.1 EpiWafer fabrication

Highly boron doped substrates with electrochemically etched porous silicon layers were provided by IMS (Insitut für Mikroelektronik Stuttgart). The 6 inch samples were sawn with a dicing saw with two horizontal cuts to a height of 10 cm. The native oxide was removed with a HF dip directly before mounting the samples in the CVD reactor RTCVD160 [6]. Subsequently, they were heated up to the process temperature of 1150 °C with a ramp of 100 K/min. Porous silicon layers were reorganized for 32 min in hydrogen atmosphere. The epitaxial layer with an average thickness of about 120 µm was grown in 75 min using trichlorosilane as precursor (5.5 g/min TCS in 11.9 slm H_2). Phosphine is used as dopant source and the flow is adjusted for a doping concentration of 3.5×10^{15} cm^{-3}. After growth samples were cooled with a ramp of 150 K/min. Edges of the final 5×5 cm^2 EpiWafers were defined with a dicing saw and detachment was prosecuted with a mechanical lift off tool developed in-house. Remaining porous silicon was removed with a chemical polish etch (CP33).

After RCA cleaning samples were passivated with Al_2O_3 layers on both sides. For defect investigation Al_2O_3 layers were removed with HF and defects were visualized using an adopted Sopori [7] solution[1].

2.2 Characterization

Average lifetimes were measured using quasi-steady-state photo conductance (QSSPC) measurements. Spatially resolved lifetimes were measured for passivated samples with photoluminescence lifetime measurements over the whole wafer area (integrated PL imaging setup, PLI [8]). On selected small areas µPL measurements [9] were applied for an investigation of the PL emission on the micron scale. Afterwards, Al_2O_3 layers were removed by an HF solution and dislocations as well as non-visible stacking faults were visualized with a Sopori etch solution [4]. Defects were investigated before and after defect etch with an optical microscope. A few defects were additionally investigated by a confocal laser microscope (Sensofar Plu S neox) to obtain structural and height information.

3 RESULTS AND DISCUSSION

To investigate the lines of reduced lifetime in EpiWafers samples with an effective lifetime of 30 to 60 µs (measured by QSSPC) and high defect densities (average density of polySF up to 11 cm^{-2}) were chosen.

[1] Here: 36 parts HF (50 %), 15 parts CH_3COOH (100 %), 2 parts HNO_3 (69 %).

3.1 Origin of lines of reduced lifetime

In Figure 1 a spatially resolved lifetime image of a 5 x 5 cm^2 sample is shown.

In the lifetime image black squares are visible corresponding to SFs mainly with polycrystalline inclusions (polySFs). Additionally, the lifetime image shows vertical and horizontal lines in <110> directions with reduced lifetimes that are not optically visible on the sample. As already discussed in [3], stacking faults are mainly situated on the crossing points of these lines. It seems likely that one is a result of the other. The question is which is cause or consequence.

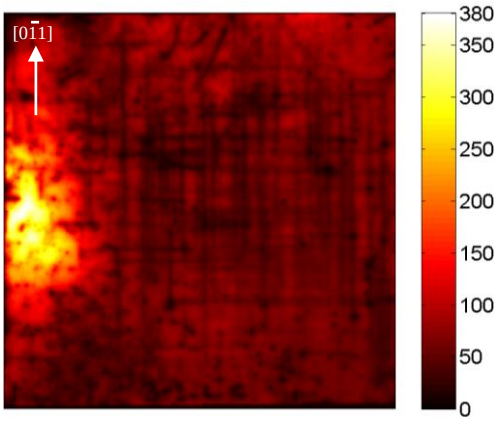

Figure 1: Lifetime image measured by PLI at ≈1 sun equivalent illumination intensity of a 5 x 5 cm^2 sample with a high defect density. Lifetimes are given in µs.

Lines of reduced lifetime could be caused by defects, particularly dislocations, that are induced by micro-scratches at the rim at elevated process temperature and move on {111} glide planes in <110> directions through the samples. This is a well-known glide system for silicon. Another explanation could be that stacking faults grow due to local disturbances of the template (e.g. crystal defects, holes or particles) and dislocations are generated at the boundary between regularly grown (100) silicon and stacking faults. Those defects could as well move through the sample on {111} glide planes leading to the line pattern of reduced lifetime.

In the first case, however, there should be more vertical then horizontal lines as only the horizontal edges of the samples are sawn causing possibly micro-cracks or other defects that in turn cause dislocations. Additionally, many lines do not extend to one of the edges of the samples as should be the case if the rim were the origin of the defects. Therefore, we conclude that defects within the epitaxially grown layer are the origin of the lines of reduced lifetime.

Taking a closer look, it can be seen that mainly polySFs are positioned at the crossing points of the afore-mentioned lines (Figure 2a). SFs without polycrystalline inclusions lead mainly to squares of reduced lifetime with the size of the SF but no surrounding line shaped features can be observed there (see Figure 2b). Thus, the following investigation focusing on the structure of the lines with reduced lifetime is restricted to the surrounding of polySFs.

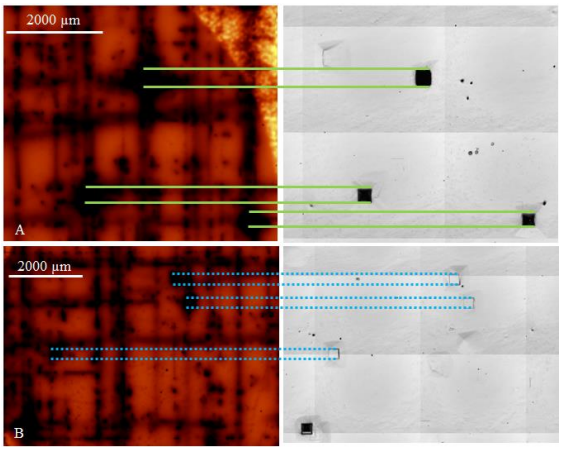

Figure 2: µPL images in arbitrary units with higher lifetime for brighter areas (left) and corresponding microscope images after defect etch (right) of selected areas of the sample shown in Figure 1. The brighter area in the upper right part of the µPL image A is a measurement artefact.

3.2 Origin for lifetime reduction at line patterns

To investigate the lines of reduced lifetime in more detail µPL images with a pixel size of 2 µm were recorded for selected polySFs and their surroundings (see Figure 3).

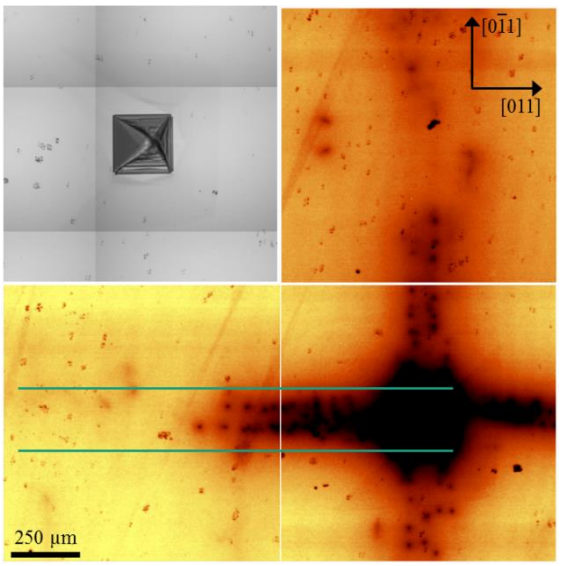

Figure 3: Picture and µPL image of a polySF and according surrounding including lines with reduced PL intensity the EpiWafer. Low PL intensity (dark) corresponds to high recombination activity. On the left side of the polySF the borders of the band in which locally reduced lifetime occurs is depicted exemplarily.

The lines visible with PLI (Figure 1) are not homogeneous in terms of lifetime. They are rather bands bordered by the edges of the polySF in which agglomerations of single dots with severely reduced lifetime are existent. Dots are often lying along two lines in <110> directions within one band. In Figure 4 the comparison of recombination activity and defect structure can be seen. Recombination within the polySF is drastically enhanced due to the polycrystalline structure (see Figure 4b) with a high defect density and most probably a high amount of impurities. The microscope

images in the lower row are taken after etching in a Sopori solution to reveal dislocations. Dislocations cumulate in the same areas in which the lifetime is reduced: within bands limited by the edges of the polySF. Since the rear surface is planar, this is better visible there (Figure 4D).

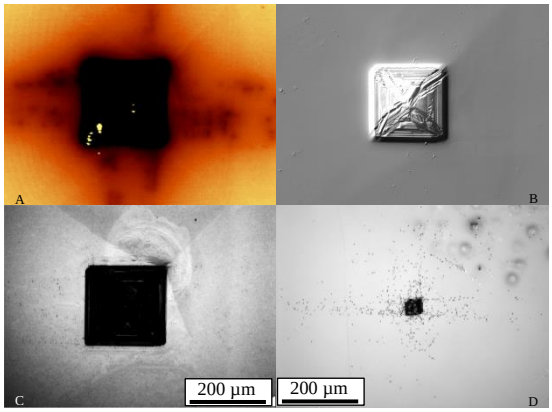

Figure 4: Images of a polySF and the surrounding area: µPL image (A), picture of the polySF taken with a confocal laser microscope (B), optical microscope pictures of front (C) and rear side of the EpiWafer after defect etch.

On front and rear side threading dislocations aligned along <110> directions are visible with increasing density near the polySF. Additionally, the shape of most etch pits is not round but with tails. Therefore, most dislocations don't break vertically through the surface. Those arguments lead to the assumption that many dislocations are lying on {111} glide planes. Such planes are bordered by an edge of the polySF on the wafer's front side and the tip of the polySF on the rear side (see scheme Figure 6).

In [4] impurities are found to be a major source for lifetime reduction in our current EpiWafer material. If an increased recombination due to a homogeneous decoration of the dislocations with impurities would be present, the dislocations should be visible as lines in the µPL image. Additionally, there seem to be many more dislocations in the microscope image than dots in the lifetime image. Therefore, we conclude that impurities agglomerate at some dislocations forming precipitates reasoning the dramatic local recombination.

3.3 Origin of dislocation structure

As already stated many dislocations are situated around polySF, most of them within bands in <110> directions bordered by the edges of the polySF. Many gather on {111} planes coinciding the edges of the polySF and the tip of the polySF. Dislocation densities around SFs without polycrystalline inclusions are much lower.

Impurities can agglomerate at grain boundaries and in areas with high defect densities which are present in the polySFs and at the interfaces between polySFs and regularly grown silicon with a (100) surface. These impurities lead to local stress during growth as well as during cool down. With µRaman measurements the Raman peak shift caused by strain in and around the polySF depicted in Figure 4 were measured (see Figure 5).

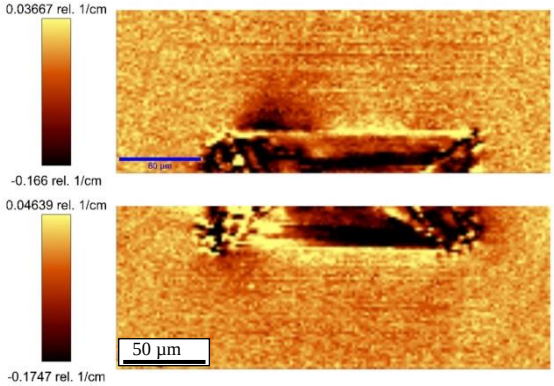

Figure 5: Local deviation from the Raman peak measured on upper and lower edge of the polySF depicted in Figure 4. A positive shift corresponds to tensile strain, a negative shift to compressive strain.

Within the polySF areas with compressive and tensile strain are visible. Within the regularly grown silicon around the polySF only small areas with compressive or tensile stress are visible. These areas are mainly located at the edges. At the corners were most dislocations seem to be generated no increased stress level can be observed. This leads to the assumption that stress is relieved by generation of dislocations. Most probable stress existing during the growth process and cool down until a certain temperature is relieved by generation of dislocations. Below that temperature thermal energy for dislocation generation is too low and strain generated during further cool down by different thermal behaviour of pure and decorated silicon cannot be relieved.

3.4 Model

Based on the observations detailed above the most probable formation mechanism of the lifetime patterns is described in the following.

At the beginning of the epitaxy process local disturbances cause growth of polySFs. Their structure and decoration with impurities lead to strain in surrounding areas during growth and cooldown. This strain is relieved by generation of dislocations that glide on {111} planes through the epitaxial layer. In Figure 6 a scheme of a polySF with {111} planes that pass through the sides of the polySF is shown. Dislocations are mainly positioned in the depicted planes and within the regions bordered by them. Therefore, bands of high dislocation density oriented in <110> directions as visible in Figure 4d can be observed. Impurities are gathered in the strain fields of these dislocations moving along the {111} planes by means of dislocation trails [10]. A part of these impurities form eventually precipitates. The high recombination activity of these precipitates arranged in bands in <110> directions primarily causes the lifetime patterns. A scheme of one poly SF with decorated areas in the (111) planes can be found in Figure 6.

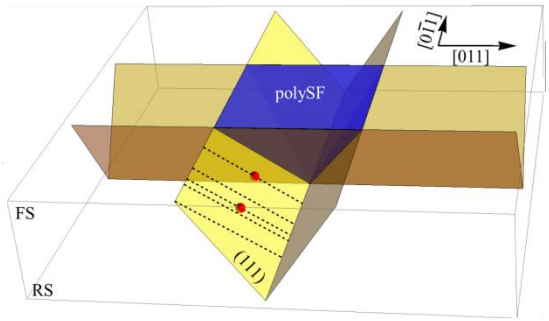

Figure 6: Scheme of a polySF with tip on the rear side (RS) and based bordered by four edges on the front side (FS). The {111} glide panes going through the sides of the polySF are depicted. Their projections on the surfaces (front and rear) are bands in <110> directions limited by the crossing of {111} planes and surfaces. On the (111) plane the assumed main position of dislocations and precipitates is shown exemplarily. Dislocations are indicated as dashed lines.

4 CONCLUSION

In lifetime images from epitaxial wafers deposited in the RTCVD160 reactor lines with reduced lifetime are visible. At the location of some crossing points of these lines the lifetime is further reduced. These locations correspond to stacking faults with polycrystalline inclusions, the most detrimental defect for local lifetimes. Close to the polycrystalline inclusions the lines are rather bands in which single spots with high recombination activity are agglomerated. In the same band high dislocation densities can be observed. We explain the observations by dislocations generated at edges and corners of the polycrystalline inclusions which move on {111} glide plains through the wafer. Impurities are gathered by the stress field of those dislocations. The high amount of dislocations and impurities around polycrystalline inclusions lead to the formation of precipitates. These precipitates with high recombination activity are aligned in <110> directions and cause the line patterns with reduced lifetime.

5 ACKNOLEDGEMENTS

The authors would like to express their gratitude to Philipp Barth, Michaela Winterhalder and Karin Zimmermann at ISE for their support and input in many valuable discussions. This work would not have been possible without the close cooperation with the NexWafe GmbH in particular with Nena Milenkovic, Kai Schillinger and Stefan Reber.
This work was funded by the German Federal Ministry for Economic Affairs and Energy (FKZ 020E-41V7452).

6 REFERENCES

[1] C. Gemmel, J. Hensen, L. David, S. Kajari-Schröder, R. Brendel, Jpn. J. Appl. Phys. 57, 041301 (2018).
[2] E. Kobayashi, Y. Watabe, R. Hao, T. S. Ravi, Prog. Photovolt: Res. Appl. 24, 1295-1303, (2016).
[3] S. Janz, D. Amiri, E Gust, S. Kühnhold-Pospischil, S. Riepe, F. Heinz, M. Drießen, Proceedings of the 33rd EUPVSEC, 343-347 (2017).
[4] P. Beu, F. Schindler, A. Fell, F. D. Heinz, D. Amiri, E. Gust, S. Janz, M. C. Schubert, IEEE Journal of Photovoltaics, under review.
[5] M.M. Kivambe et al., Journal of Crystal Growth 483, 57–64 (2018).
[6] S. Reber, C. Haase, N. Schillinger, S. Bau, A. Hurrle, Proceedings of the 3rd World Conference on Photovoltaic Energy Conversion, 1368–1371 (2003).
[7] B.L.Sopori, J. Electrochem. Soc. 131(3), p. 667-672 (1984).
[8] J.A. Giesecke, M.C. Schubert, B. Michl, F. Schindler, W. Warta, Solar Energy Materials & Solar Cells, vol. 95, 1011-1018 (2011).
[9] F.D. Heinz, L.E. Mundt, W. Warta, M.C. Schubert, Physica status solidi (RRL) 9 (12), 697–700 (2015).
[10] I.E. Bondarenko, V.G. Eremenko, B.Ya. Farber, V.I. Nikitenko, E.B. Yakimov, Phys. Stat. Sol. (b) 68, 53-60 (1981).